HEFAT2012
9th International Conference on Heat Transfer, Fluid Mechanics and Thermodynamics
16 – 18 July 2012
Malta

MODELLING THE ACTIVITY OF SEAWATER AND IMPLICATIONS FOR DESALINATION EXERGY ANALYSES

Fitzsimons L.*[1], Corcoran, B.[2], Young, P.[2], Foley, G[3]. and Regan, F[1,4].
*Author for correspondence
[1]Marine and Environmental Sensing and Technology Hub (MESTECH),
[2]School of Mechanical and Manufacturing Engineering,
[3]School of Biotechnology,
[4]School of Chemical Sciences,
Dublin City University,
Glasnevin, Dublin 9,
Ireland,
E-mail: lorna.fitzsimons@dcu.ie

ABSTRACT

Exergy analysis has been applied to desalination membrane processes in an effort to characterise energy consumption and to optimise energy efficiency. Several models have been used to this end in the literature. One assumption that is common in these analyses is that of ideal solution behavior. However, seawater and other aqueous solutions of interest do not behave ideally. Indeed, even when ideal behavior is not assumed, there are several approaches to calculate these activity values, which are typically a function of the molality and ionic strength of the electrolytic solution. What is not clear from the published literature is the impact that the choice of activity calculation model has on the exergy analysis results. The objective of this research was to undertake the exergy analysis of a seawater membrane desalination plant using the Szargut chemical exergy approach and to compare the activity calculation approaches. The chemical exergy of the seawater was calculated using several activity coefficient modelling approaches including, (a) ideal mixture model, (b) the Debye-Huckel limiting law, (c) the Davies model, and finally, (d) the Pitzer model, which is more appropriate for higher ionic strength solutions such as seawater. The results showed considerable differences in the chemical exergy rates and the magnitude of chemical exergy destruction rates calculated using the various models. For example, there were percentage differences of 61.8% and 44.7% between the magnitude of chemical exergy destruction rates calculated using the Pitzer model when compared with the Debye-Huckel limiting law for the nanofiltration and reverse osmosis processes respectively.

INTRODUCTION

Water and energy are key resources to sustain a growing population and to support economic growth. In fact, these two resources are often coupled. Generally, water is required to produce electrical power and energy is required to purify water. The current and predicted future water stress issues facing many regions are well-established [1,2]. According to the United Nations water website [3], by 2025 more than 1.8 billion people will live in regions of water scarcity and up to two thirds of the world's population could experience water stress. Consequently, water purification is becoming increasingly necessary to meet potable, industrial and agricultural water demands. However, alongside the need to conserve our vital water resources, there is also a pressing need to optimise the use of energy in water purification processes in order to mitigate environmental impacts such as climate change. From the economic perspective, the benefits of using resources efficiently are self-evident.

Exergy analysis is widely accepted as a powerful tool to characterise and optimise energy efficiency [4-9]. Several researchers have undertaken desalination plant exergy analyses [1,10-15]. However, previous research carried out by the authors has shown that the current modelling approaches (exergy calculation equations, dead state definitions, ideal mixture assumptions) can result in significantly different exergy rate and exergy destruction rate values [16,17]. Due to the choice of dead state (pure water or incoming water salinity), which is somewhat arbitrary, the differences found in the exergy rate values calculated by the various models was

expected. However, of greater importance and interest, were the significant differences that were found in the exergy destruction rate values. Primarily, these differences were due to the exergy calculation equations and the calculation of chemical exergy in particular. Differences in the chemical exergy equations can be further broken down to, (a) the varying assumptions underpinning the exergy calculation equations, (b) the calculation of the mole fractions, and (c) the assumption (or not) of ideal mixture behaviour. The exergy calculation equations were considered in detail previously by the authors [17]. Presently, the impact of the choice (or not) of ideal mixture behaviour assumption is considered. In addition, the influence of various activity coefficient calculation models is also investigated for cases when ideal mixture behaviour is not assumed. The comparison is made using a desalination process dataset from the literature [1].

The Szargut chemical exergy approach is used in this analysis and its application to water purification/desalination exergy analyses is introduced in the next section.

NOMENCLATURE

MF	Microfiltration
NF	Nanofiltration
ppm	parts per million
RDS	Restricted dead state
RO	Reverse osmosis
TDS	Total Dissolved Solids
TV	Throttling valve

Symbols:

a		Activity
α		Pitzer parameter
b		Pitzer parameter
φ		Relative humidity
ϕ		Osmotic coefficient
A		Debye-Huckel coefficient
A^{ϕ}		Pitzer coefficient
$\beta_{MX}^{(0)}$		Empirical Pitzer parameter
$\beta_{MX}^{(1)}$		Empirical Pitzer parameter
C_{MX}^{ϕ}		Empirical Pitzer parameter
$\in$		Dielectric constant
γ		Activity coefficient
c_V	[kJ/kg.K]	Specific heat capacity at constant volume
c_P	[kJ/kg.K]	Specific heat capacity at constant pressure
$\bar{e}$	[kJ/mol]	Molar chemical exergy
$\dot{E}$	[kJ/hr]	Exergy rate
$\Delta_F \bar{g}_i^{\circ}$	[kJ/mol]	Standard Gibbs energy of formation of species i
h	[kJ/kg]	Specific enthalpy
I		Ionic strength
m		Molality
$\dot{m}$	[kg/s]	Mass flow rate
$\dot{N}$	[mol/hr]	Molar flow rate
R	[kJ/mol.K]	Universal gas constant
s	[kJ/kg.K]	Specific entropy
P	[kPa]	Absolute pressure
T	[K]	Absolute temperature
ρ	[kg/m^3]	Density
v		Stoichiometric coefficient
x		Mole fraction
z		Valence

Subscripts

0	Dead state
±	Denotes activity coefficient of electrolyte rather than individual ions
aq	aqueous
Dest	Denotes exergy destruction
e	Denotes element under consideration
i	Denotes species i
ionic species	Denotes ionic species
in	In to process
M	Denotes cation
out	Out of process
sol	Denotes solution
w	Water
X	Denotes anion
NaCl	Sodium chloride

Superscripts

Ph	Physical
Ch	Chemical
∘	Standard state

EXERGY MODEL

Exergy is a thermodynamic property that combines the first and second laws of thermodynamics to determine that energy should not only be thought of in terms of quantity but also in terms of quality. Exergy can be broken down into the sum of physical (thermo-mechanical) and chemical exergy. Thermo-mechanical exergy is the maximum theoretical work that a system could do as it comes into pressure, thermal, velocity and elevation equilibrium with its environment. It is therefore a function of the difference between the pressure, temperature, velocity and elevation of the process stream at a specific thermodynamic state and the defined dead state. In the literature, this has been referred to as the restricted dead state [7]. The physical exergy rate $\dot{E}^{Ph}$ (kW) at any process stage can be calculated using (1),

$$\dot{E}^{Ph} = \dot{m}\left[h - h_0 - T_0(s - s_0)\right] \quad (1)$$

where $\dot{m}$ is the mass flow rate (kg/s), h is the specific enthalpy (kJ/kg), T is absolute temperature (K) and s is the specific entropy (kJ/kg.K), and the subscript 0 denotes the thermodynamic properties at the dead state. Using thermodynamic property relationships, and assuming that both the specific heat capacity and the density are constant, (1) can alternatively be calculated using available measurable parameters such as temperature and pressure, see (2).

$$E^{Ph} = \dot{m}\left[c_V(T - T_0) - T_0 c_P \ln\frac{T}{T_0} + \left(\frac{P - P_0}{\rho}\right)\right] \quad (2)$$

Equation (2) is the sum of thermal and pressure exergy terms, where c_V is the specific heat capacity at constant volume

(kJ/kg.K), P is the absolute pressure (kPa), ρ is the density (kg/m^3) and c_P is the specific heat capacity at constant pressure (kJ/kg.K).

The constant heat capacity assumption is very reasonable for membrane desalination processes, which are often isothermal. In this case, the thermal exergy is zero. However, the constant heat capacity assumption should be assessed for various applications of interest. The specific heat capacity relates to the specific heat capacity of the electrolytic solution.

The maximum theoretical work that a system could do at thermo-mechanical equilibrium is due to chemical exergy. In desalination exergy analyses, this generally refers to differences in concentration between the rejected brine and the local seawater environment at dead state temperature and pressure. As discussed previously, a number of different approaches have been used for desalination and other water purification applications. The approach used for this analysis is that developed by Szargut [18], which is rarely used in desalination exergy analyses. However, this approach is very interesting, particularly in respect of chemical exergy losses, i.e. streams rejected to the environment. A detailed discussion of the Szargut approach to calculate the standard chemical exergy of chemical elements and other species is beyond the scope of this paper (refer to [6,18,19]). The chemical exergy of ionic species is also discussed in detail in [17].

According to Szargut and Morris [18], the standard molar chemical exergy $\bar{e}_{sol}^{Ch}$ of solutions or mixtures can be calculated using (3) for non-ideal solutions and (4) for ideal solutions/mixtures,

$$\bar{e}_{sol}^{Ch} = \sum_i x_i \bar{e}_i^{Ch\,\circ} + RT_0 \sum_i x_i \ln a_i \tag{3}$$

$$\bar{e}_{sol}^{Ch} = \sum_i x_i \bar{e}_i^{Ch\,\circ} + RT_0 \sum_i x_i \ln x_i \tag{4}$$

where x_i is the mole fraction of the species under consideration, $\bar{e}_i^{Ch\,\circ}$ is the standard molar chemical exergy of the chemical species under consideration, R is the universal gas constant (0.0083145 kJ/mol.K) and a_i is the activity of the species under consideration. The activity takes account of the deviation from non-ideal behaviour typical of electrolytic solutions, and for the solutes, is the product of the molality and the activity coefficient. The calculation of the activity and activity coefficient is discussed later in detail.

Szargut [6,18] details two methods to calculate the standard chemical exergy of water. First, for areas under consideration that are remote from the sea, the standard molar chemical exergy of water is calculated as a function of the relative humidity φ using (5), where the subscript w denotes water and the superscript $\circ$ denotes standard temperature, pressure and standard state for solution species.

$$\bar{e}_w^{Ch\,\circ} = -RT^{\circ} \ln \varphi \tag{5}$$

The tabulated standard chemical exergy value of water is 0.9 kJ/mol, and therefore the standard relative humidity value used to calculate the chemical exergy of water is 0.696. The higher the relative humidity value, the lower the chemical exergy. For areas close to the sea, the standard chemical exergy of water is calculated using (6),

$$\bar{e}_w^{Ch\,\circ} = -RT^{\circ} \ln x_w \tag{6}$$

where x_w denotes the mole fraction of water in seawater. The standard molar chemical exergy of an electrolyte or an individual ion *i* in an aqueous solution can be calculated using (7),

$$\bar{e}_{i(aq)}^{Ch\,\circ} = \bar{e}_i^{Ch\,\circ} + \Delta_F \bar{g}_{i(aq)}^{\circ} - \Delta_F \bar{g}_i^{\circ} \tag{7}$$

where $\bar{e}_i^{Ch\,\circ}$ is the standard molar chemical exergy of the non-ionised compound or element, $\Delta_F \bar{g}_{i(aq)}^{\circ}$ is the Gibbs energy of formation of the electrolyte or ion under consideration and $\Delta_F \bar{g}_i^{\circ}$ is the Gibbs energy of formation of the compound or elements under consideration (by convention, the Gibbs energy of formation of an element at all temperatures is zero [20]), and the subscript (aq) represents aqueous. The chemical exergy of individual ions or compounds such as the bicarbonate ion can also be calculated using (8),

$$\bar{e}_{\text{ionic species}}^{Ch\,\circ} = \Delta_F \bar{g}_{\text{ionic species}}^{\circ} + \sum_e v \bar{e}^{Ch\,\circ} \tag{8}$$

where $\bar{e}_{\text{ionic speices}}^{Ch\,\circ}$ is the standard chemical exergy of the ionic species/compound under consideration, $\Delta_F \bar{g}_{\text{ionic species}}^{\circ}$ is the standard Gibbs energy of formation of the ionic species/compound, v is the stoichiometric coefficient of each element in the compound or ion and $\bar{e}^{Ch\,\circ}$ is the standard molar chemical exergy of each element, the subscript *e* refers to each of the elements under consideration. For example, the standard molar chemical exergy of the bicarbonate ion (HCO_3^-) is calculated to be -52.5 kJ/mol using (9) as follows.

$$\begin{aligned} \bar{e}_{HCO_3^-}^{Ch\,\circ} &= \Delta_F \bar{g}_{HCO_3^-}^{\circ} + \frac{1}{2}\bar{e}_{H_2}^{Ch\,\circ} + \bar{e}_C^{Ch\,\circ} + \frac{3}{2}\bar{e}_{O_2}^{Ch\,\circ} \\ &= -586.77 + \frac{1}{2}(236.1) + 410.25 + \frac{3}{2}(3.97) \end{aligned} \tag{9}$$

In the same manner the standard chemical exergy of the sodium and chloride ions and the NaCl electrolyte are 74.7 kJ/mol, -69.4 kJ/mol and 5.3 kJ/mol respectively. Values for the standard molar chemical exergy of the elements and Gibbs energy of formation were taken from [6] and [21] respectively.

SEAWATER MODEL

In the literature, seawater is often modelled as a solution/mixture of water and NaCl (ideal or non-ideal). The proportional concentration of major seawater ions are shown in Figure 1 and Figure 2, which are based on data in [22].

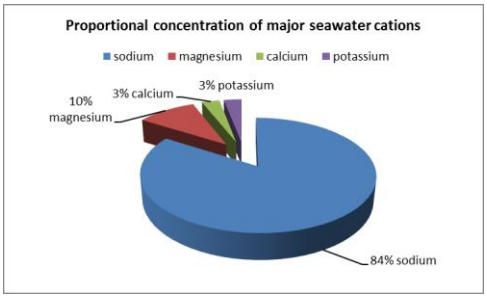

Figure 1 Proportional concentration of major seawater cations

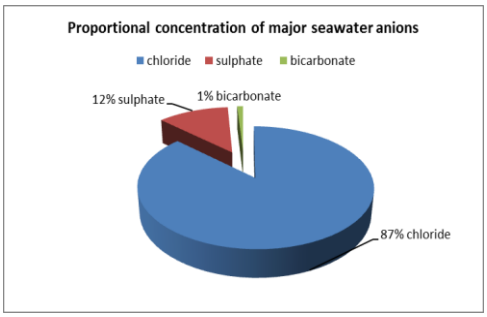

Figure 2 Proportional concentration of major seawater anions

It is evident that sodium and chloride are the major ionic species in seawater. Modelling seawater as an electrolytic solution consisting of sodium and chloride ions would appear reasonable. However, the calculation of both the ionic strength and the ionic or electrolytic activity coefficient is a function of the valence squared, and therefore, magnesium and sulphate (both divalent ions) may be more significant than their proportions alone suggest. Neglecting ions that have a mass of less than one gram per kilogram of seawater (according to data in [22]), the proportional concentration of the total major ionic constituents of seawater are shown in Figure 3.

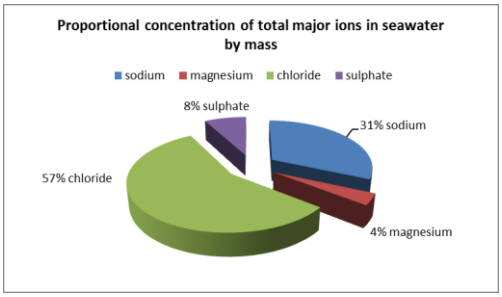

Figure 3 Proportional concentrations of total major seawater ions

However, in relation to desalination plant process stages, it is not always feasible to determine an accurate seawater analysis for multiple process stages. Electrical conductivity measurements are often used to estimate the total dissolved solids (TDS), where the electrical conductivity is multiplied by a relevant conductivity factor to determine the TDS value, which is in turn used to estimate the salt content in ppm. These factors can vary quite significantly depending on the water under consideration; values ranging from 0.55 to 0.9 are cited in the literature [23]. Furthermore, the proportionality of the ionic species is not strictly maintained in membrane processes. For example, separation by nanofiltration is considered to be a function of diffusivity and ionic charge [24], with relatively high negatively charged multivalent ionic rejection and varying monovalent ion rejection. The rejection of positively charged ions relates mainly to the size and shape of the molecule [25]. Reverse osmosis, on the other hand, rejects approximately 99% of monovalent ions and 99.6% of most divalent ions under consideration (bicarbonate is slightly less at 98.4%), see Table 1, which is adapted from [1] and reports typical rejection rates for nanofiltration and reverse osmosis desalination processes.

Ion	*NF (%)*	*RO (%)*
chloride	12.8	99
sodium	22	99
sulphate	90	99.6
magnesium	89	99.6
calcium	88.4	99.7
bicarbonate	62	98.4

Table 1 NF and RO rejection rates, adapted from [1]

Comprehensive membrane rejection rates tend to be proprietary information. To further complicate matters, the nominal rejection rates in membrane processes are a function of temperature, pressure and feedwater concentration. Therefore, it is clear that accurately modelling the individual ionic species over several process stages can be cumbersome. For this research seawater is modelled as both an NaCl electrolytic and ideal solution of varying concentrations. Future work will consider a more complete seawater model.

ELECTROLYTIC SOLUTIONS

Electrolytic solutions such as seawater do not behave ideally. However, this simplification has often been made in the literature [1,11,14,15,26-28], presumably to reduce the complexity of chemical exergy calculations. Indeed, even when ideal mixture behaviour is not assumed, there are several approaches to calculate the activity coefficient of the electrolyte under consideration [22,29-32]. Activity coefficient calculation models are primarily a function of the ionic strength of the solution, the temperature of the solution, the solvent species, and also the valence of the specific ions under consideration. The ionic strength of electrolytic solutions can be calculated using (10),

$$I = 0.5\sum m_i z_i^2 \qquad (10)$$

where m_i and z_i are the molality and valence of the species under consideration, respectively.

According to the literature [31], activity coefficient calculation models such as the Debye-Huckel limiting law, the Debye-Huckel extended equation and the Davies model [33] are not suitable for electrolytic solutions with the relatively high ionic strength of seawater (approximately 0.7 m [34,35]). Despite this, the Debye-Huckel limiting law has been used to

calculate the chemical exergy of seawater, based on the fact that seawater is a dilute solution [12].

It is evident that there are various approaches and it is unclear whether the appropriate choice of activity coefficient calculation model has an important impact on the exergy analysis results for desalination plants. Therefore, the objective of this work is to assess the impact of the ideal mixture assumption, and in the case of non-ideal mixtures, the impact of the choice of activity coefficient approach. The activity coefficient calculation equations under consideration are the Debye-Huckel limiting law [29,30], the Davies model [33] and the more accurate Pitzer activity calculation equations [36,37]. Alongside the exergy analysis of desalination plant and water purification plants, this research is also applicable to the characterisation of the theoretical work potential of salinity gradient energy generation systems.

ACTIVITY AND ACTIVITY COEFFICIENTS

The use of the activity in place of the mole fractions acknowledges the fact that electrolytic solutions do not behave ideally and accounts for the departure from ideal solution behaviour. The activity of the solutes and the solvent are calculated differently. For the solvent water, it can be calculated as a function of the osmotic coefficient ϕ, see (11),

$$\ln a_w = -\phi \frac{\nu m}{55.51} \tag{11}$$

Where ν is the number of ions generated on dissociation of the electrolyte, m is the molality (moles of solute per kilogram of water) of the electrolyte, and ϕ can be calculated using (12).

$$\begin{aligned} \phi - 1 &= -\left|z_M z_X\right| A^{\phi} \frac{\sqrt{I}}{1+b\sqrt{I}} \\ &+ m \frac{2\nu_M \nu_X}{\nu}\left[\beta_{MX}^{(0)} + \beta_{MX}^{(1)}\, \mathrm{e}^{-\alpha\sqrt{I}}\right] \\ &+ m^2\left[\frac{2(\nu_M \nu_X)^{3/2}}{\nu} C_{MX}^{\phi}\right] \end{aligned} \tag{12}$$

In the preceding equation z is the valence of the relevant ions; m is the molality of the electrolyte; I is the ionic strength of the solution; A^{ϕ} is a function of temperature, at 20°C it is 0.3882; b and α are fixed parameters, for 1-1, 2-1 and 3-1 electrolytes these values are 1.2 and 2, respectively [36,37]. The quantities $\beta_{MX}^{(0)}$, $\beta_{MX}^{(1)}$ and C_{MX}^{ϕ} are empirical parameters that are specific to the electrolyte under consideration. For NaCl at 20 °C, 1 bar, and ranging in concentration from 0-6 m, these values are reported as 0.0714, 0.2723 and 0.002, respectively [37]. Values are also reported at pressures up to 1000 bar. The pressure values of interest in this analysis range from 1-69 bar. Reported values of activity coefficient for NaCl at 0.75 M at 20 °C and 200 bar differ by approximately 1% to the values at 1 bar. Thus, at the pressures under consideration in this research, these variations are deemed negligible.

For the solutes the activity can be calculated as the product of the molality and the activity coefficient of the ionic species or electrolyte under consideration. Several activity coefficient calculation models exist and the applicability of these models as a function of ionic strength has been discussed in Stumm and Morgan [31], their analysis is reproduced here.

The Debye-Huckel model (13) is suitable for an approximate ionic strength $I < 10^{-2.3}$.

$$\log \gamma_i = -A z_i^2 \sqrt{I} \tag{13}$$

The Davies model [33] is suitable for an approximate ionic strength of $I < 0.5$, see (14). The Davies equation typically results in an error of 1.5% at an ionic strength less than 0.1 m and a 5 to 10% error at ionic strength measurements between 0.1 and 0.5 m [38].

$$\log \gamma_i = -A z_i^2 \left(\frac{\sqrt{I}}{1+\sqrt{I}} - 0.3I\right) \tag{14}$$

In the preceding equations (13) and (14), the coefficient A is a function of the dielectric constant $\in$ of the solvent and the absolute temperature and is given by (15).

$$A = 1.82\times10^{-6}(\in T)^{-\frac{3}{2}} \tag{15}$$

The dielectric constant of water $\in$, which a function of temperature, is given by (16) [39].

$$\in = 78.54\begin{bmatrix} 1-(0.004579(T-298))+ \\ (11.9\times10^{-6}(T-298)^2)+ \\ (28\times10^{-9}(T-298)^3) \end{bmatrix} \tag{16}$$

However, based on the value of seawater ionic strength (0.7 m), none of the preceding models is suitable to calculate the activity coefficient of seawater ions.

The Pitzer equations are specific interaction models and are reliable for the calculation of activity coefficients in various electrolyte solutions including seawater; they are reliable far beyond the ionic strength of seawater. Depending on the model used, the Pitzer equations can be used over the entire concentration range [40,41]. They are semi-empirical and consist of a Debye-Huckel term, which accounts for the long-range interionic effects, and several virial terms to account for short-range ionic interactions typical of electrolytic solutions. The calculation of these virial terms involves the use of several parameters including specific ion interaction terms that are fitted to measured values of various electrolytic solutions. For a single electrolyte of cation M and anion X (e.g. NaCl) the activity coefficient can be calculated using the Pitzer equation [36], see (17).

$$\begin{aligned} \ln \gamma_{\pm} &= -\left|z_M z_X\right| A^{\phi}\left[\frac{\sqrt{I}}{1+b\sqrt{I}} + \frac{2}{b}\ln(1+b\sqrt{I})\right] \\ &+ m\frac{2\nu_M \nu_X}{\nu}\left\{2\beta_{MX}^{(0)} + \frac{2\beta_{MX}^{(1)}}{\alpha^2 I}\left[1-\left(1+\alpha\sqrt{I}-\frac{\alpha^2 I}{2}\right)\mathrm{e}^{-\alpha\sqrt{I}}\right]\right\} \\ &+ \frac{3m^2}{2}\left[\frac{2(\nu_M \nu_X)^{3/2}}{\nu} C_{MX}^{\phi}\right] \end{aligned} \tag{17}$$

In (17) $\gamma_{\pm}$ is the activity coefficient of the electrolyte and the other equation parameters are identical to those defined previously in equation (12).

DESALINATION PLANT INFORMATION

The comparison of the various activity coefficient approaches was undertaken using a dataset from the literature [1]. The published information included seawater composition, nanofiltration (NF) and reverse osmosis (RO) rejection rates, temperatures, pressures and concentrations. The process stages under consideration in this analysis included various pumps, microfiltration (MF), NF, throttling valves (TV) and RO; a process schematic is shown in Figure 4. The main process parameters are shown in Table 2.

The concentration values in the final column of Table 2 can be converted to ppm values by dividing by the solution density at the various process stages. Estimated values of density for the relevant process stages, which are based on the International Equation of State for Seawater [42], and the conversion to ppm values are presented in Table 3.

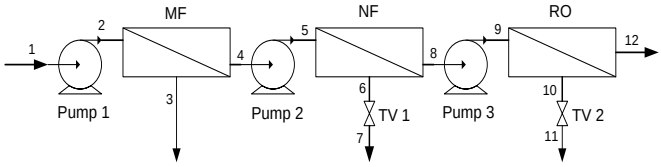

Figure 4 Process stages, adapted from [1]

Process stage	*Mass flow rate (kg/hr)*	*Temperature (K)*	*Pressure (bar)*	*Concentration (mg/l)*
1	1050000	293	1	34654
2	1050000	293	2	34654
3	55000	293	1	34654
4	995000	293	1	34654
5	995000	293	11	34654
6	245000	293	10	61852
7	245000	293	1	61852
8	750000	293	1	25733
9	750000	293	69	25733
10	231000	293	68	82567
11	231000	293	1	82567
12	516000	293	1	270

Table 2 Process parameters, adapted from [1]

Process stage	*Concentration (mg/l)*	*Estimated Density (g/l)*	*TDS (ppm)*
1	34654	1024.5	33825.3
6	61852	1045.4	59165.9
8	25733	1017.7	25285.4
10	82567	1061.6	77776.0
12	270	998.4	270.4

Table 3 Estimated density values

EXERGY RATE CALCULATION

The exergy rates and exergy destruction rates were calculated for the various desalination process stages using the Szargut chemical exergy approach. The solution was considered as both ideal and non-ideal. In relation to non-ideal behaviour the activity coefficient was calculated using a number of approaches. To summarise, the modelling approaches under consideration were;

1. Ideal solution/mixture of NaCl and water
2. The Debye-Huckel limiting law (Na and Cl ions)
3. The Davies model (Na and Cl ions)
4. The Pitzer model (NaCl electrolyte).

The physical exergy was calculated using (2). The chemical exergy rates for (a) the ideal mixture, and (b) the electrolytic solution using the Debye-Huckel limiting law and the Davies model were calculated using (18) and (19) respectively.

$$\begin{aligned}\dot{E}^{Ch} &= \dot{N}_w \bar{e}_w^{Ch} + \dot{N}_{NaCl} \bar{e}_{NaCl}^{Ch} \\ &+ RT_0 \left[\dot{N}_w \ln x_w^{RDS} + \dot{N}_{NaCl} \ln x_{NaCl}^{RDS} \right]\end{aligned} \tag{18}$$

$$\begin{aligned}\dot{E}^{Ch} &= \dot{N}_w \bar{e}_w^{Ch} + \dot{N}_{Na^+} \bar{e}_{Na^+}^{Ch} + \dot{N}_{Cl^-} \bar{e}_{Cl^-}^{Ch} \\ &+ RT_0 \left[\begin{array}{l} \dot{N}_w \ln a_w^{RDS} + \dot{N}_{Na^+} \ln \left(m\gamma \right)_{Na^+}^{RDS} + \\ \dot{N}_{Cl^-} \ln \left(m\gamma \right)_{Cl^-}^{RDS} \end{array} \right]\end{aligned} \tag{19}$$

Regarding the Pitzer model, the chemical exergy was calculated using (20).

$$\begin{aligned}\dot{E}^{Ch} &= \dot{N}_w \bar{e}_w^{Ch} + \dot{N}_{NaCl} \bar{e}_{NaCl}^{Ch} \\ &+ RT_0 \left[\dot{N}_w \ln a_w^{RDS} + \dot{N}_{NaCl} \ln \left(m\gamma \right)_{NaCl}^{RDS} \right]\end{aligned} \tag{20}$$

In (18), (19) and (20), $\dot{N}$ is the molar flow rate (mol/hr) of the relevant species, $\bar{e}^{Ch}$ is the molar chemical exergy of the relevant species (kJ/mol), x is the mole fraction, m is the molality of the electrolyte or ions, and γ is the activity coefficient of each of the species under consideration. The superscript *RDS* refers to the restricted (i.e. thermo-mechanical) dead state and the subscripts relate to the species water, the ions sodium and chloride, and the electrolyte NaCl.

Note that the Debye-Huckel limiting law and the Davies model activity coefficient calculation models calculate the activty coefficient of the individual ions whereas the Pitzer model considers the electrolyte.

The exergy destruction at the various process stages of interest (NF and RO) can be calculated using an exergy balance, see (21) below,

$$\dot{E}_{Dest} = \sum_{in} \dot{E} - \sum_{out} \dot{E} \tag{21}$$

where the rate of exergy destruction $\dot{E}_{Dest}$ is the difference between the exergy flow rates entering the process and the exergy flow rates leaving the process (modelled as a control volume in steady state). The NF and RO processes are of

primary interest because they illustrate the changes in seawater concentration and hence the chemical exergy changes.

The osmotic coefficient (12) was calculated in order to determine the activity of water (11) at each of the process stages. The activity was then compared to the corresponding mole fraction of water, see Table 4. It is evident that the activity of water and the mole fraction of water are practically identical at every process stage. Consequently, the mole fraction of water can be used without significant error, thus simplifying the relevant chemical exergy calculation equations. The general similarity of water activity and mole fraction has been previously discussed in the literature [18].

Process stage	ϕ_w	a_w	x_w
1	0.922	0.980	0.979
2	0.922	0.980	0.979
3	0.922	0.980	0.979
4	0.922	0.980	0.979
5	0.922	0.980	0.979
6	0.937	0.964	0.963
7	0.937	0.964	0.963
8	0.920	0.985	0.984
9	0.920	0.985	0.984
10	0.952	0.952	0.951
11	0.952	0.952	0.951
12	0.977	1.000	1.000

Table 4 Comparison of the activity and the mole fraction of water at the relevant process stages

RESULTS AND DISCUSSION

The physical and chemical exergy rates at each of the process stages are shown in Table 5. As reported, the physical exergy rates are positive or zero for all process stages. The value of physical exergy is zero at thermo-mechanical equilibrium. In this instance the physical exergy rate values are solely due to differences in pressure between the process stage under consideration and the dead state because the processes are isothermal. The chemical exergy rate values can be either positive or negative depending on the activity/mole fraction calculation model used.

As Table 5 shows there are large differences between the chemical exergy rates calculated using each of the approaches. The ideal mixture model and the Debye-Huckel limiting law methods result in negative values of chemical exergy for all process stages except process stage 12. The chemical exergy rates calculated using the ideal mixture model are significantly higher than the Debye-Huckel model for most process stages. They vary, in terms of ratio (ideal mixture model divided by the Debye-Huckel model), depending on the concentration at each of the process stages. For example, at process stage 8, the NF permeate stream, the value of chemical exergy rate is approximately 11 times greater than the chemical exergy rates calculated with the Debye-Huckel limiting law. However, at process stage 12, which approaches ideal behaviour, the ratio is almost unity (0.98). The difference in values is solely due to the difference between the mole fraction of NaCl and the activity of the solutes (i.e. the sodium and chloride ions).

Process stage	*Physical exergy rate (kJ/hr)*	*Chemical exergy rate (kJ/hr)*			
		Ideal mixture	*D-H limiting law*	*Davies model*	*Pitzer model*
1	0	-4985172	-953701	822590	3750477
2	102489	-4985172	-953701	822590	3750477
3	0	-261128	-49956	43088	196454
4	0	-4724044	-903745	779502	3554023
5	971205	-4724044	-903745	779502	3554023
6	210924	-1866909	-570965	621997	1684432
7	0	-1866909	-570965	621997	1684432
8	0	-2584595	-242798	489213	2105350
9	5011300	-2584595	-242798	489213	2105350
10	1457894	-2093635	-753599	1137794	2324618
11	0	-2093635	-753599	1137794	2324618
12	0	1402878	1428026	1427341	1440757

Table 5 Physical and chemical exergy rates – comparison of chemical exergy rates calculated using the various models

The chemical exergy rates are positive for the Davies and Pitzer models but again there are notable differences between the values. The Pitzer model is 4.5 times greater than the Davies model for process stage 1, and again, due to ideal behaviour, is very similar to the ideal mixture, Debye-Huckel and Davies models at process stage 12.

In general, the Szargut approach results in relatively large values of chemical exergy when compared to other approaches because it includes both a standard chemical exergy value and an 'entropy of mixing' term. Alternate approaches typically calculate chemical exergy as a function of the dead state temperature and the natural logarithm of the ratio of the activities of the species under consideration, i.e. the ratio of the activity of the relevant species at the restricted dead state (*RDS*) at the concentration of the process stage of interest and the activity of the species at the defined dead state $RT_0 \ln(a_i^{RDS} / a_i^{DS})$. However, the Szargut standard chemical exergy terms cancel out in the exergy analysis of processes where no chemical reaction takes place and the chemical exergy destruction is then solely a function of the dead state temperature and the entropy of mixing terms. However, where the Szargut approach is particularly interesting is the quantification of exergy losses to the environment. In the case of seawater desalination plants, these are the brine streams (process stages 7 and 11). The Szargut model assigns an intrinsic value to these streams, which accounts for the energy input to purify the water in the solution and the intrinsic chemical exergy of the electrolyte.

Of greater interest, in terms of energy efficiency, are the process exergy destruction rates and these are presented for the key separation processes (NF and RO) and the two throttling valves (TV1 and TV2) in Table 6.

Process	*Physical exergy destruction (kJ/hr)*	*Chemical exergy destruction(kJ/hr)*			
		Ideal mixture	*D-H limiting law*	*Davies model*	*Pitzer model*
NF	760281	-272540	-89982	-331708	-235759
TV1	210924	0	0	0	0
RO	3553406	-1893838	-917225	-2075922	-1660026
TV2	1457894	0	0	0	0

Table 6 Physical and chemical exergy destruction rates – comparison of chemical exergy destruction rates calculated using the various models

The physical exergy destruction is due to pressure dissipation across the membranes and the throttling valves. According to Table 6, the highest physical exergy destruction occurs in the RO process followed by the second throttling valve. The chemical exergy destruction is, as expected, zero for the throttling valves as no change in concentration, and hence chemical exergy, takes place. However, the chemical exergy destruction rates are negative for the key membrane separation processes. This finding is interesting. The negative chemical exergy destruction values may be viewed as off-setting the pressure exergy destruction associated with membrane processes, i.e. the total exergy destruction rates, which include the sum of the thermal, pressure and chemical exergy destruction, are reduced by adding the negative value of chemical exergy destruction. When the physical and chemical exergy rates are not decoupled these negative values go unnoticed.

However, for the purposes of the model comparison, the negative exergy destruction values are considered as a magnitude and are shown for the NF and RO processes in Figure 5.

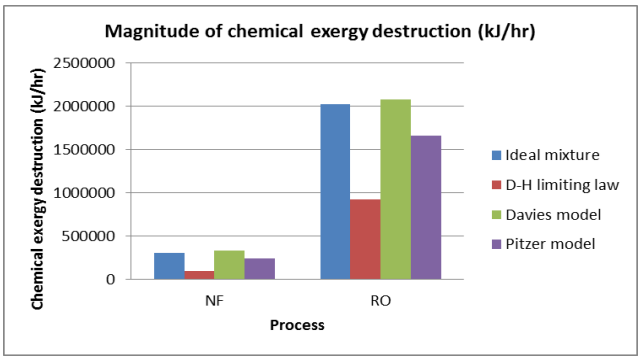

Figure 5 Comparison of chemical exergy destruction calculated using the four models

It is clear from Figure 5 that the magnitude of chemical exergy destruction is highest when calculated using the Davies model for both processes. These values are similar to the ideal mixture model (the Davies model is greater than the ideal mixture model for the NF and RO processes by factors of 1.2 and 1.1 respectively). The chemical exergy destruction is significantly lower for the Debye-Huckel limiting law model (the Davies model is greater than the Debye-Huckel model for the NF and RO processes by approximate factors of 4 and 2 respectively). In comparison to the Davies model, the Pitzer model differs for the NF and RO processes by factors of 1.4 and 1.25 respectively. These are interesting findings, which again are solely due to the choice of activity/mole fraction calculation approach.

The Pitzer model is an accurate basis for calculating the activity of electrolytic solutions, and therefore, should be the most accurate approach. The use of this model results in lower values of magnitude of chemical exergy destruction than either the Ideal mixture or Davies models but significantly higher levels than the Debye-Huckel limiting law for both separation processes. The percentage difference values between each of the other three models and the Pitzer model are quantified in Table 7.

Based on these findings, it is evident that the choice of activity calculation model, or indeed, the assumption of ideal mixture behaviour, has a significant impact on the values of chemical exergy and chemical exergy destruction rates obtained, and therefore, should be an important consideration for researchers undertaking exergy analyses.

Process	*% Diff. vs. Ideal mixture model*	*% Diff. vs. D-H limiting law*	*% Diff. vs. Davies model*
NF	-27.9	61.8	-40.7
RO	-21.7	44.7	-25.1

Table 7 Percentage difference between the magnitude of chemical exergy destruction rates calculated using the Pitzer model versus the Ideal mixture, D-H limiting law and the Davies models for the NF and RO processes

CONCLUSIONS

This research used the Szargut chemical exergy model approach to undertake the exergy analysis of a seawater desalination plant. Following a detailed literature review, this approach has not been applied to desalination exergy analyses previously.

One of the key objectives of this research was to investigate the impact of ideal/non-ideal behaviour assumptions and to assess the various activity calculation models for electrolytic solutions. Four models were assessed, (a) the ideal mixture/solution model, (b) the Debye-Huckel limiting law, (c) the Davies model, and (d) the Pitzer model. The Pitzer model is considered the most accurate method to calculate the activity of electrolytic species at the ionic strengths of the solutions considered in this research. It was found that the various models resulted in significant differences in chemical exergy rates and chemical exergy destruction rates for the two key separation processes (reverse osmosis and nanofiltration). For example, there were percentage differences of 61.8% and 44.7% between the magnitude of chemical exergy destruction rates calculated using the Pitzer model when compared with the Debye-Huckel limiting law for the nanofiltration and reverse osmosis processes respectively. Therefore, it is evident that the

choice of activity calculation model has important implications for desalination exergy analyses, and indeed, salinity gradient energy systems.

Future work will consider and compare the Szargut/ Pitzer model approach with an electrolytic exergy model/Pitzer model approach and consider a more comprehensive seawater electrolytic model.

ACKNOWLEDGEMENTS

Grateful acknowledgements go to the Irish Research Council for Science, Engineering and Technology (IRCSET) for funding part of this research. In addition, the authors would like to acknowledge the Marine and Environmental Sensing Technology Hub (MESTECH), which is funded under the Beaufort Marine Research Awards and carried out under the Sea Change Strategy and the Strategy for Science Technology and Innovation (2006-2013), with the support of the Marine Institute, funded under the Marine Research Sub-Programme of the National Development Plan 2007–2013.

REFERENCES

[1] E. Drioli, E. Curcio, G. Di Profio, F. Macedonio, A. Criscuoli, Integrating membrane contactors technology and pressure-driven membrane operations for seawater desalination: Energy, exergy and costs analysis, Chem.Eng.Res.Design. 84 (2006) 209-220.
[2] M.A. Shannon, P.W. Bohn, M. Elimelech, J.G. Georgiadis, B.J. Marinas, A.M. Mayes, Science and technology for water purification in the coming decades, Nature. 452 (2008) 301-310.
[3] United Nations website, Water for Life, 2011, [on-line], (Accessed 2011).
[4] J.E. Ahern, The Exergy Method of Energy Systems Analysis, John Wiley & Sons, Canada, 1980.
[5] T.J. Kotas, The Exergy Method of Thermal Plant Analysis, Krieger Publishing Company, Florida, 1995.
[6] J. Szargut, Exergy Method - Technological and Ecological Applications, WIT Press, Southampton, U.K., 2005.
[7] A. Bejan, Advanced Engineering Thermodynamics, John Wiley & Sons, New Jersey and Canada, 2006.
[8] M.J. Moran, H.N. Shapiro, Fundamentals of Engineering Thermodynamics, Wiley, England, 2006.
[9] I. Dincer, M.A. Rosen, Exergy: energy, environment and sustainable development, Elsevier, U.K.; U.S.A., 2007.
[10] K.S. Spiegler, Y. El-Sayed, The energetics of desalination processes, Desalination. 134 (2001) 109-128.
[11] Y. Cerci, Exergy analysis of a reverse osmosis desalination plant in California, Desalination. 142 (2002) 257-266.
[12] J. Uche, Themoeconomic Analysis and Simulation of a Combined Power and Desalination Plant, (2000), PhD thesis, Universidad de Zaragoza, Spain.
[13] V. Romero-Ternero, L. Garcia-Rodriguez, C. Gomez-Camacho, Thermoeconomic analysis of a seawater reverse osmosis plant, Desalination. 181 (2005) 43-59.
[14] N. Bouzayani, N. Galanis, J. Orfi, Thermodynamic analysis of combined electric power generation and water desalination plants, Appl.Therm.Eng. 29 (2009) 624-633.
[15] A.S. Nafey, H.E.S. Fath, A.A. Mabrouk, Exergy and thermoeconomic evaluation of MSF process using a new visual package, Desalination. 201 (2006) 224-240.
[16] L. Fitzsimons, B. Corcoran, P. Young, G. Foley, A Comparison of Prevalent Desalination Exergy Models, (2010), 19-21 July, 7th International Conference on Heat Transfer, Fluid Mechanics and Thermodynamics (HEFAT 2010), Antalya, Turkey.
[17] L. Fitzsimons, A Detailed Study of Desalination Exergy Models and their Application to a Semiconductor Ultra-Pure water Plant, (2011), PhD thesis, Dublin City University, Ireland.
[18] J. Szargut, D.R. Morris, F.R. Steward, Exergy Analysis of Thermal, Chemical and Metallurgical Processes, Hemisphere, New York, 1988.
[19] J. Szargut, A. Valero, W. Stanek, A. Valero, Towards an International Legal Reference Environment, (2005).
[20] C.E. Housecroft, A.G. Sharpe, Inorganic Chemistry, Pearson Education Ltd., England, 2007.
[21] D.D. Wagman, W.H. Evans, V.B. Parker, NBS Tables of Chemical Thermodynamic Properties: Selected values for inorganic and C1 and C2 organic substances in SI units, American Chemical Society and the American Instituute of Physics for the National Bureau of Standards, Washington D.C. 1982.
[22] F.J. Millero, Chemical Oceanography, CRC Press, Florida, United State, 2005.
[23] C.N. Sawyer, P.L. McCarty, G.F. Parkin, Chemistry for Environmental Engineering, McGraw-Hill, Singapore, 1994.
[24] M. Cheryan, Ultrafiltration and Microfiltration, Technomic Publishing Company, Inc., Pennsylvania, United States of America, 1998.
[25] A.I. Schafer, A.G. Fane, T.D. Waite, Nanofiltration Principles and Applications, Elsevier, Oxford, U.K., 2005.
[26] N. Kahraman, Y.A. Cengel, B. Wood, Y. Cerci, Exergy analysis of a combined RO, NF, and EDR desalination plant, Desalination. 171 (2005) 217-232.
[27] F. Macedonio, E. Drioli, An exergetic analysis of a membrane desalination system, Desalination. 261 (2010) 293-299.
[28] N. Bouzayani, N. Galanis, J. Orfi, Comparative study of power and water cogeneration systems, Desalination. 205 (2007) 243-253.
[29] P. Debye, E. Huckel, Physik. Z. 24 (1923) 185-334.
[30] P. Debye, E. Huckel, Physik. Z. 25 (1924) 97.
[31] W. Stumm, J.J. Morgan, Aquatic Chemistry, John Wiley & Sons Inc., New York, 1996.
[32] G.N. Lewis, M. Randall, Thermodynamics, McGraw-Hill, United States, 1961.
[33] C.W. Davies, Ion Association, Butterworths, London, 1962.
[34] J. Szargut, D.R. Morris, CALCULATION OF THE STANDARD CHEMICAL EXERGY OF SOME ELEMENTS AND THEIR COMPOUNDS, BASED UPON SEA WATER AS THE DATUM LEVEL SUBSTANCE, Bulletin of the Polish Academy of Sciences: Technical Sciences. 33 (1985) 293-305.
[35] R. Rivero, M. Garfias, Standard chemical exergy of elements updated, Energy. 31 (2006) 3310-3326.
[36] K.S. Pitzer, Thermodynamics of electrolytes. I. Theoretical basis and general equations, J.Phys.Chem. 77 (1973) 268-77.
[37] K.S. Pitzer, J.C. Pelper, R.H. Busey, Thermodynamic Properties of Aqueous Sodium Chloride, Journal of Physical Chemistry reference Data. 13 (1984).
[38] I.N. Levine, Physical Chemistry, McGraw-Hill, New York, 2002.
[39] H. Harned, B. Owen, The Physical Chemistry of the Electrolyte Solution, Reinhold, New York, 1958.
[40] S.L. Clegg, K.S. Pitzer, P. Brimblecombe, Thermodynamics of multicomponent, miscible, ionic solutions. Mixtures including unsymmetrical electrolytes, J.Phys.Chem. 96 (1992) 9470-9479.
[41] S.L. Clegg, K.S. Pitzer, Thermodynamics of multicomponent, miscible, ionic solutions: generalized equations for symmetrical electrolytes, J.Phys.Chem. 96 (1992) 3513-3520.
[42] UNESCO website, International Equation of State of Seawater, 1980, [on-line], (Accessed 2009).